ChemBioChem

Research Article
doi.org/10.1002/cbic.202300755

Chemistry Europe
European Chemical Societies Publishing

www.chembiochem.org

Heterochiral modifications enhance robustness and function of DNA in living human cells

Tracy L. Mallette,[a] Diane S. Lidke,[b] and Matthew R. Lakin*[c]

Oligonucleotide therapeutics are becoming increasingly important as more are approved by the FDA, both for treatment and vaccination. Similarly, dynamic DNA nanotechnology is a promising technique that can be used to sense exogenous input molecules or endogenous biomarkers and integrate the results of multiple sensing reactions *in situ* via a programmed cascade of reactions. The combination of these two technologies could be highly impactful in biomedicine by enabling smart oligonucleotide therapeutics that can autonomously sense and respond to a disease state. A particular challenge, however, is the limited lifetime of standard nucleic acid components in living cells and organisms due to degradation by endogenous nucleases. In this work, we address this challenge by incorporating mirror-image, L-DNA nucleotides to produce heterochiral "gapmers". We use dynamic DNA nanotechnology to show that these modifications keep the oligonucleotide intact in living human cells for longer than an unmodified strand. To this end, we used a sequential transfection protocol for delivering multiple nucleic acids into living human cells while providing enhanced confidence that subsequent interactions are actually occurring within the cells. Taken together, this work advances the state of the art of L-nucleic acid protection of oligonucleotides and DNA circuitry for applications *in vivo*.

Introduction

Nucleic acid nanotechnology is an exciting platform whose advances are likely to benefit a number of fields, including biomedical diagnostics and therapeutics. In this context, the combinatorial, sequence specific chemistry of nucleic acids offers a powerful mechanism for programming the behavior of molecules and cells, with the ultimate goal of diagnosing and/or treating a disease state. Oligonucleotide therapeutics are short nucleic acid polymers which have a range of mechanisms of operation and are among the most commercially successful applications of nucleic acid nanotechnologies. Antisense oligonucleotides (ASOs) are typically 17–25 nucleotides long and are designed to modulate gene expression through target sequence binding.[1] ASOs were the first type of oligonucleotide to receive FDA approval and currently there are multiple drugs approved as well as in the FDA pipeline in this classification.[2] Other important classes of oligonucleotide therapeutics include small interfering RNA (siRNA),[3] CRISPR-based therapeutics,[4] and vaccines which can target cancer or infectious diseases.[5,6] An important property that all of these therapeutics have in common is that they must be chemically modified in order to survive *in vivo* and perform their desired functions.[7]

Chemical modifications are designed into nucleic acids in order to enhance their resistance to nuclease-mediated degradation. They can be incorporated into the backbone, sugar, or bases. Phosphorothioate linkages are made by replacing an oxygen with sulfur in the nucleotide backbone and are widely used in oligonucleotide therapeutics.[9] Another common modification occurs at the 2′ position of the ribose sugar by substituting the hydroxyl group with O-methyl (2′-OMe), O-methoxyethyl (2′-MOE) or fluoro (2′-F) groups.[2] When these modifications are put on the flanking regions of the strand, the resulting oligonucleotides are referred to as "gapmer" ASOs.[2] Alternative nucleic acids such as peptide nucleic acid (PNA)[10] and locked nucleic acid (LNA)[11] have also been incorporated into therapeutic oligonucleotides.

Dynamic DNA nanotechnology is a subfield of nucleic acid nanotechnology in which programmed interactions are carried out on recognized input molecules to produce designed outputs, e.g., to mimic the behavior of decision-making tasks such as the evaluation of logic operations.[12] Integrating dynamic DNA nanotechnology with oligonucleotide therapeutics could allow for the development of highly specific smart therapeutics, in which a "smart drug" can not only sense its biochemical environment and make diagnostic decisions but also act autonomously on those decisions to treat the disease state. However, the challenges of component delivery to cells and degradation of components within cells have limited the deployment of DNA nanotechnology for such applications in living cells and organisms.[13] Much of the DNA nanotechnology work carried out in cells to date has relied on the same chemical modification strategies as outlined above.[14,15] Detection of endogenous microRNA (miRNA) and signal processing in

[a] *Dr. T. L. Mallette*
Center for Biomedical Engineering,
University of New Mexico,
Albuquerque, New Mexico, 87131, USA

[b] *Dr. D. S. Lidke*
Department of Pathology and Comprehensive Cancer Center,
University of New Mexico School of Medicine,
Albuquerque, New Mexico, 87131, USA

[c] *Dr. M. R. Lakin*
Department of Computer Science, Department of Chemical & Biological Engineering, Center for Biomedical Engineering, University of New Mexico,
Albuquerque, New Mexico, 87131, USA
E-mail: mlakin@cs.unm.edu

Supporting information for this article is available on the WWW under https://doi.org/10.1002/cbic.202300755

living cells has been demonstrated[16,17] as well as conditional activation of an siRNA.[14] Importantly, some of the chemical modifications used have been shown to significantly change the reaction kinetics.[18,19] Recently, however, ourselves and others have pioneered a novel approach to enhancing nuclease resistance for intracellular DNA nanotechnology: the use of mirror-image, left-handed (L-) nucleotides (Figure 1a).

Naturally occurring nucleic acids (DNA and RNA) have a double helix which twists to the right, and are thus referred to as D-DNA or D-RNA, respectively. Nucleases have evolved to recognize naturally occurring D-nucleic acids and are enantiospecific, which means that the enantiomer L-DNA is highly resistant to nuclease degradation (Figure 1b,c), as demonstrated in our previous work.[8,20] Due to the chiral mismatch, L-DNA does not bind to D-DNA according to the conventional rules of Watson-Crick DNA base-pairing.[21] This can be advantageous in terms of minimizing off-target effects of a synthetic L-DNA oligonucleotide in a biological system, however, it poses a challenge for designing the interface between an L-DNA probe and a D-nucleic acid target. This challenge can be overcome by using an L-nucleic acid aptamer, though these must be isolated on a case-by-case basis.[22] Other alternatives include achiral PNA intermediates[23] and heterochiral strands containing both D- and L-DNA.[8,20,24] An additional advantage of L-DNA for the development of oligonucleotide therapeutics is its relatively low immunogenicity compared to more exotic chemical modifications applied to D-nucleic acids.[25]

Once any nucleic acid nanotechnology has been designed to survive in the cell, the next issue that must be addressed is how to deliver it into the cell. A benefit of some of the chemical modifications, like phosphorothioate linkages and LNA, is that they allow gymnotic uptake of "free" oligonucleotides.[26] Other common delivery methods require forming complexes between the oligonucleotide and a delivery agent, ligands, nanoparticles, or lipids, in order to increase the rate of endocytosis and are often tailored to the delivery destination.[27] A common delivery agent is the lipid molecule cholesterol, which can be incorporated as a DNA modification and which has been shown to improve uptake of both oligonucleotides and larger DNA nanostructures into cells.[28,29] An interesting intersection between oligonucleotide therapeutics and DNA nanotechnology is the use of relatively large DNA origami nanostructures as a way to deliver cargo, including therapeutics, to the cell.[30] A majority of the work done to date with dynamic DNA nanotechnology has used lipid-based transfection agents to deliver the components, but there have been issues with poor colocalization with separate deliveries so cotransfection was used.[14,31]

Our goal in this work is twofold: (1) to validate heterochiral DNA nanotechnology reactions in living mammalian cells as a viable technology for future development of nucleic acid therapeutics and (2) to develop and optimize sequential lipid-based transfection protocols for circuit delivery to demonstrate long-term survival of components within cells. Inspired by our previous work using model biological fluids *in vitro*,[8] we use L-DNA as a flanking protective modification, which we refer to as a "toecap", on a D-DNA oligonucleotide to form a heterochiral gapmer oligonucleotide (Figure 1c). We use toehold-mediated strand displacement (TMSD) reactions as an assay to measure the intactness of this strand (L TC X) by its ability to react with a reporter complex (R) and increase fluorescence due to loss of Förster resonance energy transfer (FRET) between fluorophore and quencher modifications on that reporter (Figure 1d). We developed a transfection protocol to test this reaction in living mammalian cells in a way that provides enhanced assurance that the reaction is actually occurring inside the cell and not during the transfection process, for example. Using this approach, we show that our heterochiral gapmer approach also provides protection for oligonucleotides in living cells, as well as in model systems *in vitro*. Our work thus advances the state of the art of intracellular DNA nanotechnology and validates a novel modification strategy

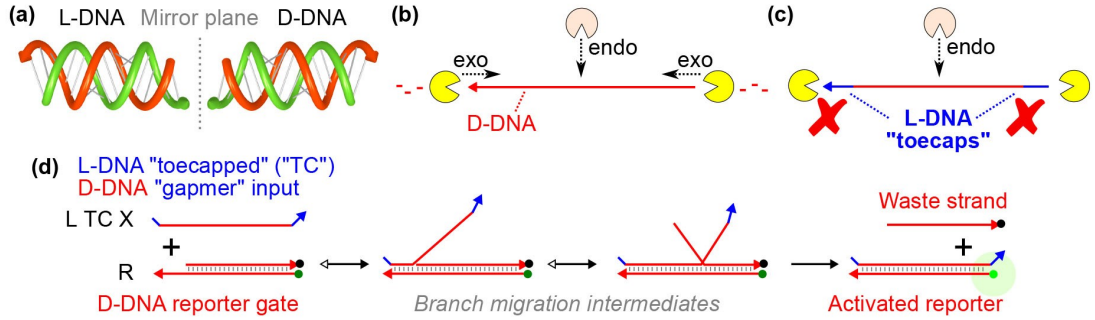

Figure 1. Heterochiral DNA for *in vivo* dynamic DNA nanotechnology. (a) L-DNA is the chiral mirror image of naturally occurring D-DNA. (b) *In vivo*, homochiral D-DNA oligomers are susceptible to degradation by cellular exo- and endonucleases. (c) Heterochiral gapmer oligomers, in which a central D-DNA domain is flanked by protective L-DNA "toecaps", resist degradation by exonucleases, although they may still be susceptible to degradation by endonucleases that can directly attack the D-DNA domain. (d) Heterochiral oligonucleotides can be used to implement DNA strand displacement reactions, in which an input oligonucleotide binds to a double-stranded gate via a short exposed complementary toehold domain; the input then initiates a random walk branch migration process which is enthalpically biased toward the completed state shown on the right, in which the input is bound to the bottom strand of the reporter gate and the top strand from the gate is now displaced and freely diffusing in solution. The progress of this reaction can be tracked via loss of FRET from a labeled reporter gate due to separation of the quencher (covalently linked to the top strand) from the fluorophore (covalently linked to the bottom strand). The system shown here can accept both a homochiral D-DNA input or a heterochiral "gapmer" input whose strand termini are protected by short L-DNA domains that we refer to as "toecaps", to protect them from degradation by exonucleases.[8]

and testing method that may also impact future development of oligonucleotide therapeutics.

Results and Discussion

Characterization of test system *in vitro*

In order to test the effectiveness of a protective L-DNA toecap in living cells, we designed a simple model system consisting of a one-step toehold-mediated strand displacement (TMSD) reaction (Figure 1d). The system comprises a homochiral D-DNA reporter (R) for observing the output and accepts an input strand that is either a D-DNA strand protected with an L-DNA "toecap" consisting of five adenine bases (L TC X), as introduced in our previous work,[8] or a homochiral D-DNA control (X). Either input is able to displace the quencher strand from the reporter complex, which is labeled with a Cy5/quencher FRET pair. We also designed an off-target negative control input (Y) that is the same length as X but not able to activate Y via strand displacement. This is an important control when we are working with living cells to ensure that all cells are exposed to the same total amount of exogenous DNA during the experiment; computational predictions confirmed negligible interaction of the Y strand with the component strands of the reporter gate R. This system should be able to demonstrate a difference in response between protected and non-protected input strands while being simple enough to be transfected effectively into living mammalian cells. We first tested the system in pristine conditions in buffer and confirmed that the protected (L TC X) and non-protected (X) inputs perform similarly at activating the reporter gate (R), while the off-target input (Y) causes minimal reporter activation (Figure 2a).

We next tested this reporter system in a mock biological fluid of 10% fetal bovine serum (FBS) and 40% Dulbecco's Modified Eagle Medium (DMEM) in order to expose the system to a range of nucleases. System inputs and an off-target D-DNA control were incubated in 10% FBS with 40% DMEM at 37 °C for 18 hours. After the incubation period, the reporter complex was spiked into the reaction and then monitored on a plate reader for three hours. Figure 2b shows that using an input to reporter ratio of 5× gives a strong signal from the protected input while the non-protected, homochiral D-DNA input is only slightly above the negative control. This is consistent with our previous work[8] and we interpret this to mean that the L-DNA toecap is indeed able to protect the input and reduce the degradation during the initial incubation period. We used an excess of input because the cytoplasm of a mammalian cell is a crowded and spatially complex environment and it is thus likely that not all of the intact input strands will encounter the reporter complex during the timespan of our experiments. It is also worth noting that there is an increase in fluorescence from the untriggered reporter in the negative control when exposed to 10% FBS as compared to the buffer experiment, which we attribute to degradation of the D-DNA reporter itself (Figure 2). This still allows for a three fold increase in the TC input condition, which is a large enough dynamic range to be confident that the reaction did occur.

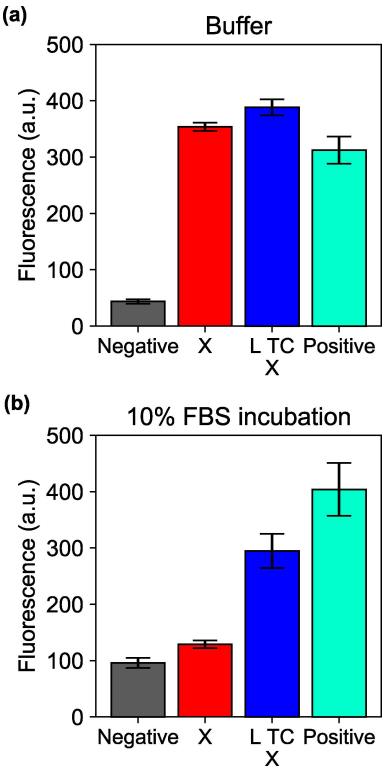

Figure 2. Plate reader fluorescence data comparing the performance of protected versus non-protected inputs in a one-step TMSD reaction. (a) Endpoint of reaction in TE Mg^{2+} buffer reaction after three hours. In these pristine conditions, the signals from the reporter and off-target input (Negative) both remain low while the two inputs reach similar levels of fluorescence. Inputs were at 5× the concentration of the reporter complex. Error bars are the standard deviation of three technical replicates. (b) Test of the same conditions in a mock biological fluid with active enzyme degradation. Inputs were incubated in 10% FBS with 40% DMEM at 37 °C for 18 hours. After incubation, the reporter complex was spiked into the reaction and then monitored on a plate reader for three hours. For both tests, reporter concentration was 300 nM (1×) and the off-target input (Y) was added to the negative control at the same 5× concentration as the input cases (X and L TC X).

Sequential transfection confirms strand displacement in living cells

Given these data, we developed a plan for testing the system in living cells. A human cell line, HeLa, was chosen for the work due to its relevance to future biomedical applications. Previous work on DNA nanotechnology in cells co-transfected the circuit components,[14,31] but this method makes it difficult to determine whether the reaction is truly happening inside the cell or if components are reacting before or while entering the cell. Furthermore, previous control experiments to determine whether complexation with lipid-based transfection reagents can prevent TMSD reactions from occurring have produced

contradictory and thus inconclusive results.[14,31] In order to conclusively demonstrate that the reaction is actually happening in the cell, as well as to test the long term stability of the toecapped input, we chose to perform two sequential, lipid-based transfections (Figure 3).

We first confirmed that the cells would tolerate the sequential transfections by using two DNA complexes with different unconditionally fluorescent labels (Figure S1); we observed that cells can survive two lipid-based transfections and also that the efficiency of the co-transfection for each fluorophore was similar to the efficiency from sequential transfection for that fluorophore. We next used an acid stripping protocol to confirm that the observed fluorescently labeled strands were not merely adhered to the outer cell membrane post-transfection (Figure S2). Acid stripping was not included in the final reaction protocol in order to reduce time between the final transfection and the flow cytometry reading, but the results do confirm that not only can the cells tolerate our sequential transfection protocol but also that the protocol did in fact deliver the DNA cargo into the interior of the cells, as intended. We also determined that different fluorophores have different transfection efficiencies and thus we chose to use Cy5 as our reporter fluorophore in subsequent experiments (Figure S3).

D-DNA reporter leak contributes to measured fluorescence

Our next sequential transfection experiment aimed to understand the background fluorescent signal from our negative control, thus, we tested a homochiral L-DNA reporter and a homochiral D-DNA reporter with the same sequence and fluorophore-quencher pair. In the negative control experiments, each reporter was tested with an off-target input in the first transfection as detailed in the Electronic Supplementary Information, so that the total amount of DNA was consistent with our other experiments. This means that there should be no strand displacement and any observed signal should be from reporter leak. We expected to observe a higher fluorescent signal from the D-DNA negative control because L-DNA is naturally resistant to nuclease degradation and will not degrade during the experiment, but some amount of D-DNA degradation should occur.

When compared to untransfected cells, we observed an increase in the fluorescent signal from the L-DNA negative control (L-DNA reporter with off-target D-DNA input) as shown in Figure 4. As a fully L-DNA reporter should be robust to enzymatic degradation, we believe this nominal signal shows the quenching efficiency of our FRET pair.[32] As predicted, the D-DNA negative control (D-DNA reporter with off-target D-DNA input) shows a much higher signal increase than the L-DNA negative control (Figure 4). We theorize that the D Negative signal represents the addition of the quenching efficiency and, crucially, the degradation of the D-DNA causing separation of the two strands of the reporter complex. Given this needed measure of short term degradation of the system reporter, we used the D-DNA reporter with an off target input as our negative control in subsequent experiments to distinguish the signal caused by reporter activation from the signal caused by leak. The negative control signal varies in each experiment, likely due to biological variation and environmental factors.

L-DNA toecaps enhance stability in living cells

We then used the test protocol, outlined in Figure 3, to determine if the improved signal we saw *in vitro* from the toecapped input after incubation would be present when tested in living cells. Transfections for all single strands and complexes were done with a commercially available lipid-based transfection reagent as described in the Electronic Supplementary Information. The input was transfected first and after two hours the media was removed and the cells were washed with phosphate buffered saline (PBS) twice, to remove any input

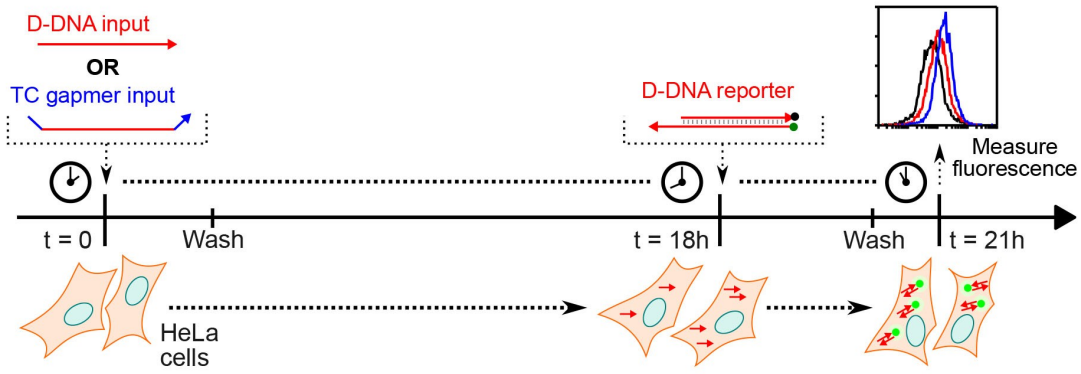

Figure 3. Sequential transfection protocol for strand displacement reactions in living human cells. Homo- or heterochiral input oligonucleotides were transfected via lipid-based transfection at time zero and washed two hours later to remove any input DNA from the surrounding media or from the outer surfaces of cell membranes. Cells were incubated until t = 18 h and then transfected again with the corresponding strand displacement reporter gate. After a further 2 h incubation the cells were washed again and fluorescence was measured by flow cytometry at t = 21 h, to measure completion of the strand displacement reaction. The negative control consisted of a similar reaction but with an off-target D-DNA input transfected at time zero (not shown in image).

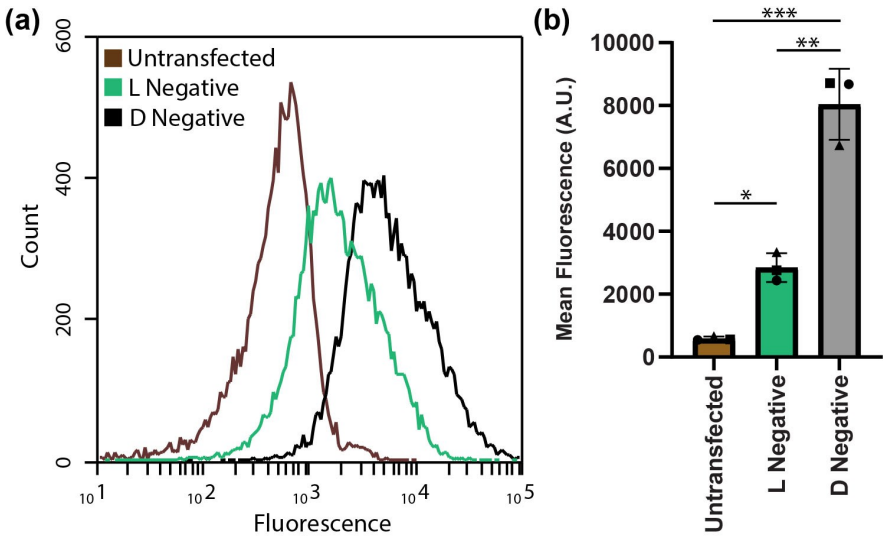

Figure 4. Comparison of homochiral L-DNA and D-DNA reporter signal in living cells. (a) Histogram of cell count versus fluorescence in the Cy5 channel. The L-DNA reporter plus off-target D-DNA input (L Negative, green) shows an increase in fluorescent signal compared to untransfected cells (brown). The D-DNA reporter plus off-target D-DNA input (D Negative, black) shows a further increase in fluorescent signal indicating more leak (positive signal in the absense of input). (b) Average mean fluorescence value of three true replicates from different days along with standard deviation. The difference between each condition is significant as calculated by two-way ANOVA and Fisher's Least Significant Difference test.

strands remaining in the surrounding media. After the transfection, the cells were incubated for an additional 16 hours in complete DMEM before the reporter complex was transfected following the same protocol. Flow cytometry data was taken three hours after the beginning of the reporter transfection, that is, 21 hours after the beginning of the experiment, which mirrors the endpoint of the plate reader data shown in Figure 2.

As a positive control for fluorescent signal strength in these experiments, an unconditionally fluorescent gate (reporter complex without the quencher) was transfected in equal amounts as the reporter in the input plus reporter experiments. The fluorescence values obtained by this control only require successful transfection of a single fluorescently-labeled complex to produce a fluorescent signal. In a multi-component system, however, the likelihood of all components being available to complete the TMSD reaction is expected to decrease exponentially with the number of separate required transfection events, so it is not surprising that for the TMSD system comprising an input and a reporter, the fluorescence will be significantly lower than for a single unconditionally fluorescent complex. In addition, previous work has shown that after cellular uptake, oligonucleotides can be trapped in endosomes or lysosomes and not all escape into the cytosol.[33] Fluorescent labels, like the Cy5 on the reporter complex, have also been found to have unique colocalization patterns.[34] These effects are thus expected to further reduce the fluorescent signal generated by our two-component TMSD system. Therefore, instead of a true prediction of reaction completion, this control provides an upper bound for the maximum possible observable fluorescence. Consequently, it is reassuring that the fluorescence signals observed from all of our input conditions fall between the negative and positive control bounds (Figure 5).

We tested three different input to reporter dose ratios to study the sensitivity of the system as well as to find the best observation regime for the L-DNA toecap protection. Different input ratios change the total amount of DNA transfected as well as the overall DNA concentration which we hypothesized may change the burden on the cell, its response to the transfection, and the sequestration of nucleases or other cofactors. These changes may be expected to influence the resulting rates of degradation of the transfected components. We tested a 5:1 input:reporter ratio (the test condition used *in vitro)*, a 2.5:1 ratio, and equal stoichiometry (1:1 ratio). The histogram of the first run is shown as an example histogram for each input ratio case (Figure 5, left). For the 5:1 and 2.5:1 conditions, flow cytometry data show that in both input cases (X and L TC X) there is a statistically significant increase in mean fluorescent signal over the negative control condition (Figure 5a, b, middle). This confirms that the programmed TMSD reactions are occurring inside the cell. More importantly, for 5:1 and 2.5:1, the increase in mean fluorescence over negative is greater for the L-DNA toecap protected input L TC X than the homochiral D-DNA control input X (Figure 5a, b, middle). In the 1:1 condition, there is still an increase for the input cases over negative and again, the L TC X input shows a higher signal than the unprotected input X, however, these relationships were not found to be statistically significant. This aligns with previous work[14] and we believe the weaker signal is caused by decreased likelihood of multiple components co-locating in the cells when lower concentrations of input are present (Figure 5c). These results highlight the challenges in accurately quantitating

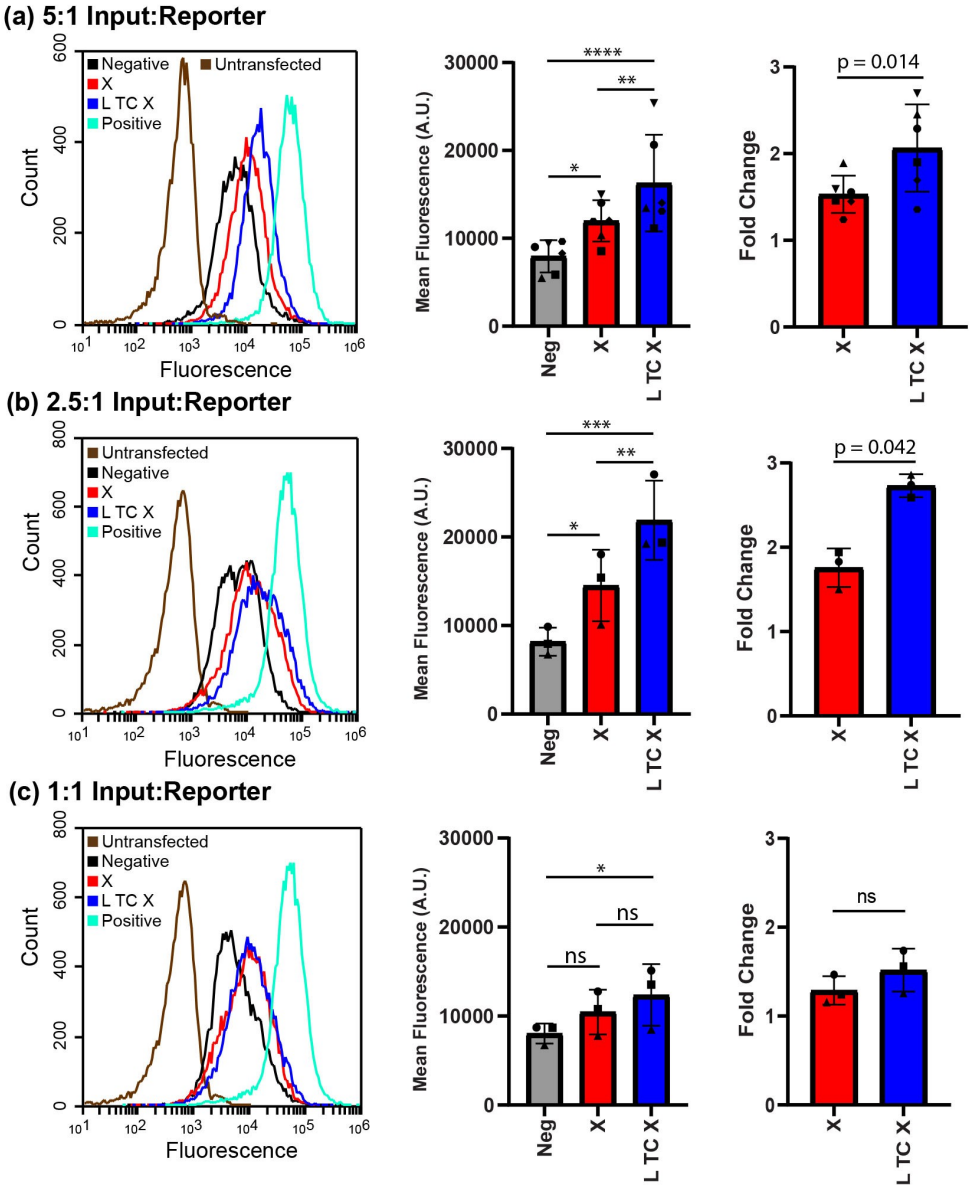

Figure 5. Flow cytometry results showing strand displacement reporter activation in living cells. Left, an example histogram of Cy5 channel fluorescence and cell count from the first run of each experimental condition including the untransfected and positive controls. Middle, plot of average mean fluorescence and standard deviation for different inputs: off-target (Neg); unprotected, homochiral D-DNA input (X); L-DNA protected, triblock heterochiral input (L TC X). Right, fold change of mean fluorescence of on target inputs (X and L TC X) over off-target (Neg). (a) 5:1 Input:Reporter ratio and (b) 2.5:1 Input:Reporter ratio show a significant increase in signal from on-target to off-target as well as from protected to unprotected. (c) 1:1 Input:Reporter ratio shows low or no significance between input conditions. All replicates are true replicates and significance statistics were calculated using two-way ANOVA and Fisher's Least Significant Difference test.

the stability and performance of DNA computing components in transfected mammalian cells.

The mean fluorescence of the input conditions was converted to the fold change over the negative control so that multiple days of experiments could be compared while compensating for some of the inherent variability associated with experiments involving living, cultured mammalian cells (Figure 5, right). For the 5:1 ratio, the L TC X input achieves a 2.1 ± 0.46 fold increase over negative which is 35% higher than the fold change seen with the unprotected input X (1.5 ± 0.20 fold). For the 2.5:1 ratio, the L TC X input achieves a 2.7 ± 0.11 fold increase over negative which is 55% higher than the fold change seen with the unprotected input X (1.8 ± 0.19 fold). Both increases were found to be statistically significant ($p = 0.0104$ and $p = 0.042$, respectively). It is interesting that the 2.5:1 ratio showed a larger increase in fold change for the

L-DNA toecap protected input compared to the unprotected input than the 5:1 ratio. We hypothesize that the 2.5:1 ratio may be high enough to saturate the reporter and increasing the amount of DNA beyond this ratio diminishes the reaction because of the additional stress of transfection on the cells. Our results show that a sequential transfection protocol can be used to study long-term behavior of dynamic DNA nanotechnology in living cells and that L-DNA toecaps can improve the longevity of single-stranded DNA oligonucleotides in the intracellular environment.

To study the distribution of circuit components within the transfected cells, confocal images of live cells were also taken. Cells were plated in an 8-well chamber, as described in the Electronic Supplementary Information and the transfections were performed as outlined in Figure 3 with input and reporter complex amounts scaled to the lower cell count. Figure 6 shows representative live cell images, with green representing Cy5 fluorescence. The top row from left to right contains a wide field view of cells transfected with the negative control (Y), non-toecapped (X), and toecap-protected (L TC X), respectively. These images show the increase in fluorescence from the reporter both in the number of cells containing fluorescence and the intensity of fluorescence in each cell. The bottom images are higher magnification images taken from a different field of view in the same experiment shown on the top row, in each case. The activated reporter puncta are largely in the cytoplasm, but some signal is also seen inside the nucleus, especially for cells with a high number of activated reporter complexes. This pattern is consistent with previous studies done on the trafficking of oligonucleotides inside the cell and could be driven by association with a number of proteins.[27]

Enhanced performance of L TC X is due to toecap chirality

Finally, we set out to confirm that the observed improvement in robustness was coming from the left-handed chirality of the protective toecap. To test this hypothesis, we repeated the sequential transfection protocol at a 5:1 ratio with an additional input, D TC X, where the same protective toecap sequences were added as before, but this time as D-DNA. As before, the L TC X input shows a significantly higher signal than the

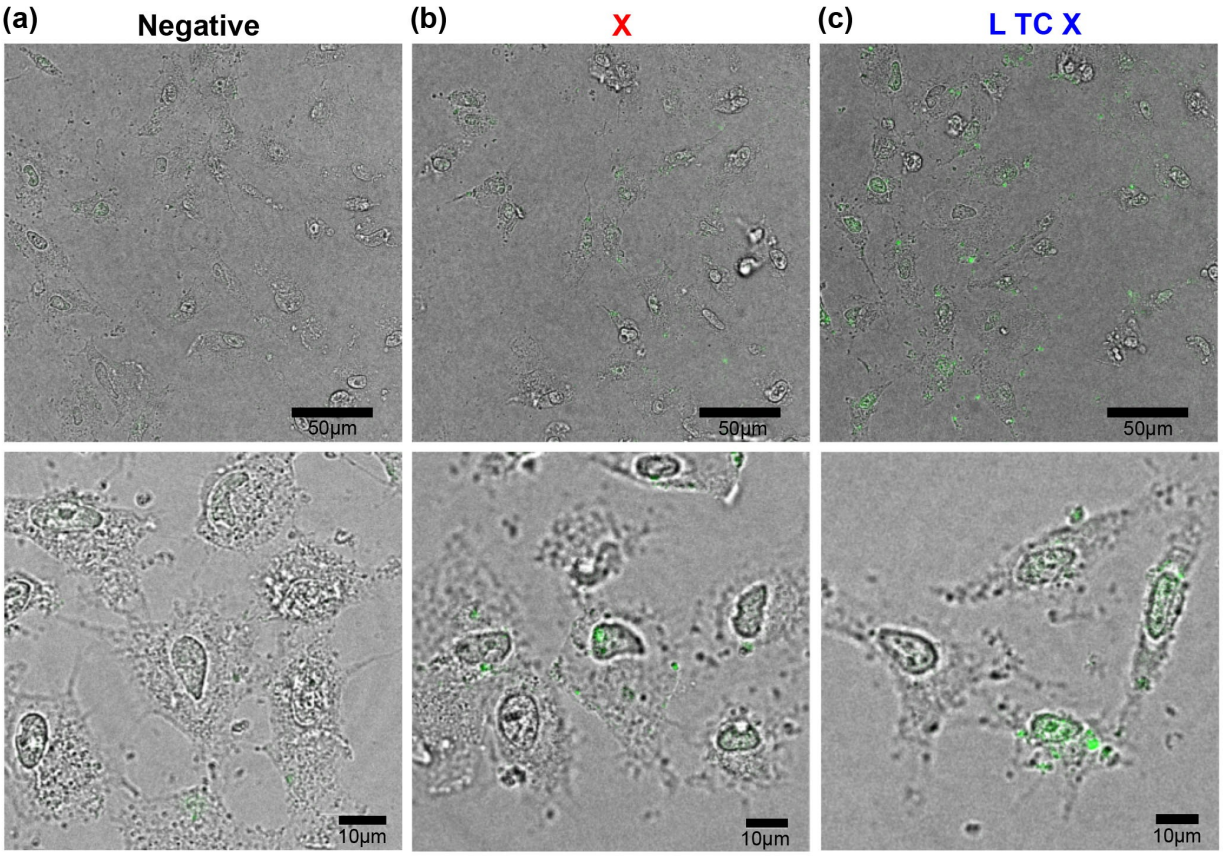

Figure 6. Representative confocal fluorescence microscopy images of reporter activation in HeLa cells for a 5:1 input to reporter ratio. (a) Negative control with reporter and off-target input (Y) shows low levels of reporter activation. (b) The non-toecapped input (X) shows some activation of the reporter complex. (c) The toecapped input (L TC X) shows the greatest level of activation. Cy5 fluorescence is shown in green and the intensity was scaled relative to the brightest L TC X level observed. Images taken on Leica TCS SP8 Confocal microscope, transfections were performed as described in Figure 3 and cells were plated on an 8-well chamber slide as described in the material and methods. Bottom images were taken in separate view fields.

unprotected input X, and notably, the L TC X signal is also significantly higher than the D-DNA protected input (D TC X, Figure 7). The L TC X signal had a 2.5±0.27 fold increase over negative which was a 64% increase over the unprotected input X (1.5±0.18) and a 38% increase over the D-DNA protected D TC X (1.8±0.19). There is a small increase in signal seen between X and D TC X, which may be because longer DNA strands take longer to be degraded by nucleases. This increase is not significant when comparing mean fluorescence, though the increase in fold change (19%) was shown to be significant (both tested through two-way ANOVA and Fisher's Least Significant Difference).

Previous work has shown that some cyanine dyes have an increased intensity when adjacent DNA is rich in adenine bases.[35] As the toecap is a 5 nucleotide poly-A sequence, we tested if this effect is observable for our system. We did find this effect to be a large contributor to signal brightness for *in vitro* tests of the system in buffer regardless of chirality, (Figure S4). However, Figure 7 supports that this effect is not significant enough in living cells to overcome the effects of degradation. Furthermore, our previous work has shown that other toecap sequences can be used with similar effects,[8] which could be used in future experiments in mammalian cells where cyanine dyes are beneficial for enhanced transfection efficiency. Overall, the results of comparing the D-DNA toecap to the L-DNA toecap support our hypothesis that left-handed chirality is necessary for improved signal.

Conclusions

In conclusion, we have established a protocol for sequential transfection of dynamic DNA nanotechnology components which provides stronger assurance that programmed interactions between those components, such as strand displacement reactions, are in fact occurring within the cells. We confirmed the feasibility of this procedure by testing with two labeled components to determine that preferential transfection was not an issue. Additionally, acid stripping verified that the components were inside the cell membrane. While we showed an improved method for two component delivery, there is still a need for better transfection reagents and protocols, especially focused on reliable delivery of multi-component molecular circuits into cells. Further work to improve control of the stoichiometries of components would enable us to transfect more complex multi-component nucleic acid circuits, which are capable of more sophisticated intracellular information processing.

Most importantly, we have demonstrated that flanking L-DNA toecaps are effective at protecting a heterochiral gapmer from exonuclease degradation in living human cells. We made this observation using a strand displacement assay for gapmer intactness and monitoring resulting fluorescence through flow cytometry and confocal microscopy. The best signal increase was shown at a 2.5:1 input to reporter ratio, though the L-DNA protection increased observed signal at all tested input to reporter ratios. We confirmed that the protection is due to the left-handed chirality of the toecap, not from the increased input length or sequence based fluorophore effects. Previous studies have suggested that L-oligonucleotides have low immunogenicity,[25] however recent work has indicated that this may not be universally true.[36] Further investigation could be done into the protection conferred by different length toecaps and sequences, along with their immunogenicity, to inform the best way to use these motifs. Future work could also combine the toecaps with other chemical modifications to further protect against endonucleases. Our work therefore shows that flanking L-nucleic acids

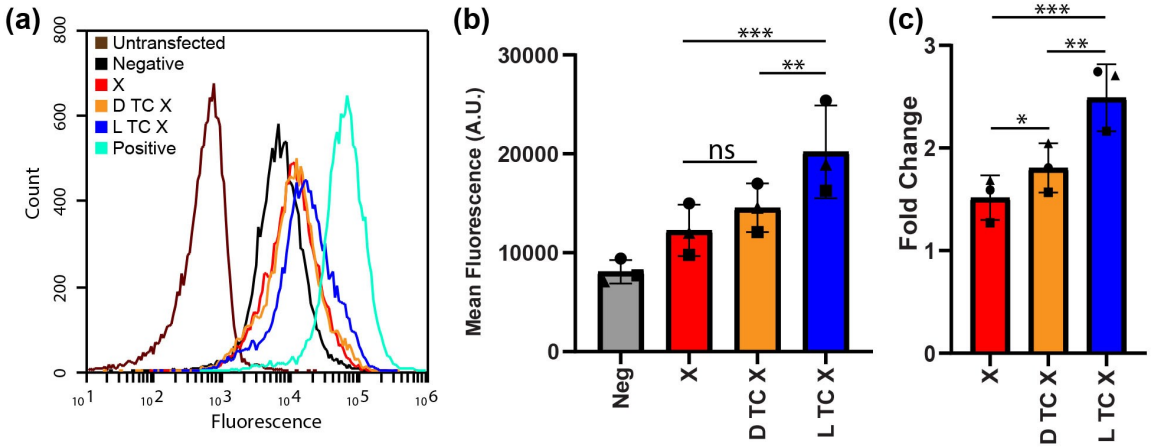

Figure 7. Comparison of D-DNA and L-DNA toecaps. (a) Representative histogram of cell count versus fluorescence in the Cy5 channel from the first run of the experiment including the untransfected and positive controls. (b) Plot of average mean fluorescence and standard deviation for different inputs: off-target (Neg); unprotected, homochiral D-DNA input (X); input with additional D-DNA toecaps, (D TC X), L-DNA protected, triblock heterochiral input (L TC X). The homochiral D-DNA inputs are not significantly different while the L-DNA toecap shows significant signal increase compared to the homochiral D-DNA inputs. (c) Fold change of mean fluorescence of on target inputs (X, D TC X, and L TC X) over off-target (Neg). The L-DNA protected input shows the highest fold change. All replicates are true replicates and significance statistics were calculated using two-way ANOVA and Fisher's Least Significant Difference test.

can be a powerful tool in the design of oligonucleotide therapeutics as well as intracellular dynamic DNA nanotechnology systems, which could have practical applications including the autonomous diagnosis and treatment of disease.

Author Contributions

Conceptualization: T.L.M., D.S.L., M.R.L. Funding acquisition: D.S.L., M.R.L. Investigation: T.L.M. Methodology: T.L.M., D.S.L., M.R.L. Supervision: D.S.L., M.R.L. Visualization: T.L.M., M.R.L. Writing – original draft: T.L.M., D.S.L., M.R.L. Writing – review and editing: T.L.M., D.S.L., M.R.L.

Acknowledgements

This material is based upon work supported by the National Science Foundation under Grants 1763718 and 2044838. Additional support came from the National Institutes of Health under Grant R35 GM126934. We sincerely thank Shayna Lucero for assistance with cell culture and gratefully acknowledge use of the University of New Mexico Cancer Center fluorescence microscopy and flow cytometry facilities, as well as NIH-NCI support via P30CA118100 for this core.

Conflict of Interests

The authors declare the following competing financial interest(s): A patent application has been filed on this research.

Data Availability Statement

The data that support the findings of this study are available from the corresponding author upon reasonable request.

Keywords: Heterochiral DNA · HeLa cells · Robustness · Toehold-mediated strand displacement · Transfection

[1] A. Aartsma-Rus, L. van Vliet, M. Hirschi, A. A. M. Janson, H. Heemskerk, C. L. de Winter, S. de Kimpe, J. C. T. van Deutekom, P. A. C. 't Hoen, G.-J. B. van Ommen, *Mol. Ther.* **2009**, *17*, 548.
[2] T. C. Roberts, R. Langer, M. J. A. Wood, *Nat. Rev. Drug Discovery* **2020**, *19*, 673.
[3] J. J. Valdés, A. D. Miller, *Sci. Rep.* **2019**, *9*, 16146.
[4] Y. K. Dhuriya, A. A. Naik, *Mol. Biol. Rep.* **2023**, *50*, 1845.
[5] N. Pardi, M. J. Hogan, F. W. Porter, D. Weissman, *Nat. Rev. Drug Discovery* **2018**, *17*, 261.
[6] A. Batista-Duharte, L. Sendra, M. J. Herrero, D. Téllez-Martínez, I. Z. Carlos, S. F. Aliño, *Biomolecules.* **2020**, *10*, 316.
[7] C. Rinaldi, M. J. A. Wood, *Nature Reviews Neurology* **2018**, *14*, 9.
[8] T. L. Mallette, M. R. Lakin, *ACS Synth. Biol.* **2022**, *11*, 2222.
[9] F. Eckstein, *Nucleic Acid Ther.* **2014**, *24*, 374.
[10] J. Saarbach, P. M. Sabale, N. Winssinger, *Curr. Opin. Chem. Biol.* **2019**, *52*, 112.
[11] R. N. Veedu, J. Wengel, *RNA Biol.* **2009**, *6*, 321.
[12] G. Seelig, D. Soloveichik, D. Y. Zhang, E. Winfree, *Science* **2006**, *314*, 1585.
[13] Y.-J. Chen, B. Groves, R. A. Muscat, G. Seelig, *Nat. Nanotechnol.* **2015**, *10*, 748.
[14] B. Groves, Y.-J. Chen, C. Zurla, S. Pochekailov, J. L. Kirschman, P. J. Santangelo, G. Seelig, *Nat. Nanotechnol.* **2016**, *11*, 287.
[15] J. Fern, R. Schulman, *ACS Synth. Biol.* **2017**, *6*, 1774.
[16] J. Hemphill, A. Deiters, *J. Am. Chem. Soc.* **2013**, *135*, 10512.
[17] X. Gong, J. Wei, J. Liu, R. Li, X. Liu, F. Wang, *Chem. Sci.* **2019**, *10*, 2989.
[18] D. Y. Zhang, E. Winfree, *J. Am. Chem. Soc.* **2009**, *131*, 17303.
[19] X. Olson, S. Kotani, B. Yurke, E. Graugnard, W. L. Hughes, *J. Phys. Chem. B* **2017**, *121*, 2594.
[20] T. L. Mallette, M. N. Stojanovic, D. Stefanovic, M. R. Lakin, *ACS Synth. Biol.* **2020**, *9*, 1907.
[21] K. Hoehlig, L. Bethge, S. Klussmann, *PLoS One* **2015**, *10*, e0115328.
[22] A. M. Kabza, J. Sczepanski, *ChemBioChem* **2017**, *18*, 1824.
[23] A. M. Kabza, B. E. Young, J. T. Sczepanski, *J. Am. Chem. Soc.* **2017**, *139*, 17715.
[24] B. E. Young, J. T. Sczepanski, *ACS Synth. Biol.* **2019**, *8*, 2756.
[25] A. M. Kabza, N. Kundu, W. Zhong, J. T. Sczepanski, *WIREs Nanomedicine and Nanobiotechnology* **2021**, *14*, e1743.
[26] H. S. Soifer, T. Koch, J. Lai, B. Hansen, A. Hoeg, H. Oerum, C. A. Stein, Silencing of Gene Expression by Gymnotic Delivery of Antisense Oligonucleotides, in M. Kaufman, C. Klinger (Editors), *Functional Genomics: Methods and Protocols*, vol. 815 of *Methods in Molecular Biology*, chapter 25, pages 333–346, Springer **2012**.
[27] R. L. Juliano, *Nucleic Acid Ther.* **2018**, *28*, 166.
[28] P. Chaltin, A. Margineanu, D. Marchand, A. V. Aerschot, J. Rozenski, F. D. Schryver, A. Herrmann, K. Müllen, R. Juliano, M. H. Fisher, H. Kang, S. D. Feyter, P. Herdewijn, *Bioconjugate Chem.* **2005**, *16*, 827.
[29] W. L. Whitehouse, J. E. Noble, M. G. Ryadnov, S. Howorka, *Bioconjugate Chem.* **2019**, *30*, 1836.
[30] P. Wang, M. A. Rahman, Z. Zhao, K. Weiss, C. Zhang, Z. Chen, S. J. Hurwitz, Z. G. Chen, D. M. Shin, Y. Ke, *J. Am. Chem. Soc.* **2018**, *140*, 2478.
[31] W. Zhong, J. T. Sczepanski, *ACS Synth. Biol.* **2021**, *10*, 209.
[32] S. A. E. Marras, F. R. Kramer, S. Tyagi, *Nucleic Acids Res.* **2002**, *30*, e122.
[33] K. Deprey, N. Batistatou, M. F. Debets, J. Godfrey, K. B. VanderWall, R. R. Miles, L. Shehaj, J. Guo, A. Andreucci, P. Kandasamy, G. Lu, M. Shimizu, C. Vargeese, J. A. Kritzer, *ACS Chem. Biol.* **2022**, *17*, 348.
[34] A. Lacroix, E. Vengut-Climent, D. de Rochambeau, H. F. Sleiman, *ACS Cent. Sci.* **2019**, *5*, 882.
[35] N. Kretschy, M. Sack, M. M. Somoza, *Bioconjugate Chem.* **2016**, *27*, 840.
[36] C.-H. Yu, J. T. Sczepanski, *Chem. Sci.* **2023**, *14*, 1145.

Manuscript received: December 19, 2023
Accepted manuscript online: January 16, 2024
Version of record online: February 12, 2024